Weierstraß-Institut
für Angewandte Analysis und Stochastik

im Forschungsverbund Berlin e.V.

Preprint ISSN 0946 – 8633

Compression limit by third-order dispersion in the normal dispersion regime

Ayhan Demircan[1], Marcel Kroh[2], Uwe Bandelow[1], Bernd Hüttl[2], Hans-Georg Weber[2]

submitted: 14 March 2006

[1] Weierstrass Institute
for Applied Analysis and Stochastics
Mohrenstraße 39
10117 Berlin, Germany
E-Mail: demircan@wias-berlin.de
bandelow@wias-berlin.de

[2] Fraunhofer-Institute for Telecommunications
Heinrich-Hertz-Institute
Einsteinufer 37
10587 Berlin,Germany
E-Mail:kroh@hhi.de
huettl@hhi.fraunhofer.de
hgweber@hhi.fhg.de

No. 1108
Berlin 2006

2000 *Mathematics Subject Classification.* 35Q55,35Q60.

Key words and phrases. Nonlinear Schrödinger Equation, Optical Fiber.

This work was supported by the state Berlin and the EU under the Grant TOB B1-1911.

Edited by
Weierstraß-Institut für Angewandte Analysis und Stochastik (WIAS)
Mohrenstraße 39
10117 Berlin
Germany

Fax: + 49 30 2044975
E-Mail: preprint@wias-berlin.de
World Wide Web: http://www.wias-berlin.de/

Abstract

Broad-band continua at gigahertz rates generated in high-nonlinear dispersion flattened fibers in the normal dispersion regime near the zero-dispersion wavelength can be used for a subsequent efficient pulse compression, leading to stable high-repetition-rate trains of femtosecond pulses. We show experimentally and theoretically that third-order dispersion defines a critical power, where beyond further compression is inhibited. This fundamental limit is caused by a pulse-breakup.

1 Introduction

High-repetition-rate optical pulse trains for ultrahigh-speed optical time-divison multiplexed communication systems require stable femtosecond optical pulse sources in the 1550 nm regime. Since low jitter pulses that are directly obtainable from typical semiconductor laser based pulse sources are still limited to approximately 1 ps in duration, an external compression scheme must be employed to generate a femtosecond optical pulse train with gigahertz repetition rate [1, 2]. Efficient compression can be achieved by taking advantage of the nonlinear properties of optical fibers. In the anomalous dispersion regime the propagation dynamics of higher-order solitons leads to an extreme narrowing of the pulse width [3]. But the inherent third-order dispersion (TOD) in these fibers can result in significant disadvantage on the soliton-effect pulse compression scheme [4], by imposing an oscillatory structure at the back end of the pulse and a splitting of the main peak into two peaks [5]. Another effective method for pulse compression is the nonlinear pulse evolution in a fiber with normal group-velocity dispersion (GVD) followed by an anomalous dispersive medium [6]. The key step here is to take advantage of the ability of the wider bandwidth generated by SPM to support a shorter pulse. It is well known that this compression scheme also suffers by TOD and it is believed that a compensation or a reduction of TOD will permit the delivery of clean pulses. In this letter we show that even a small amount TOD can lead to a pulse break-up above a certain pulse power, which represents a fundamental limit to the compression scheme.

2 Experimental setup

The experimental setup is shown in Fig. (1). A tunable mode-locked laser (EC-MLL) was used to generate pulse trains with a repetition rate of 10 GHz with timing jitter smaller than 100 fs (between 100 Hz – 10 MHz), and 1535–1565 nm tuning range. The direct output of the EC-MLL was amplified in a high-power erbium-doped fiber amplifier (EDFA), which has a maximum average output power of 26 dBm. A pulse with a $sech^2$ form is then propagated through a highly nonlinear fiber (HNLF) with a dispersion flattened profile to minimize the TOD. The dispersion and its slope at 1550 nm is approximately $D = -0.09\,ps/nm/km$ and $S = 0.019\,ps/nm^2/km$, respectively. The HNLF has its zero dispersion wavelength (ZDW) centered at $\lambda = 1555$ nm. The fiber is 789 m long and has a nonlinear coefficient of $\gamma = 10.5\,W^{-1}km^{-1}$, with a fiber loss of $0.84\,dB/km$. The chirped pulse is launched into a standard single mode fiber (SMF) for a subsequently recombining of the frequency components leading to the desired compression. The spectral characterization of the pulses is obtained with an optical spectrum analyzer. Parallely the technique of frequency-resolved optical gating (FROG) [7] is used to characterize the intensity and the frequency chirp of the pulses propagating through the HNLF .

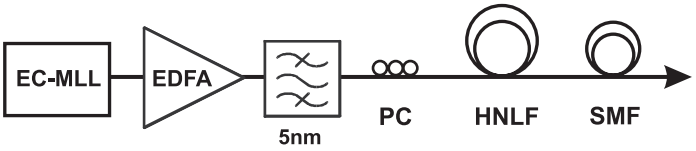

Figure 1: Experimental setup used for pulse compression (abbreviations are defined in the text).

3 Numerical modeling

We have solved numerically the one-dimensional generalized nonlinear Schrödinger equation (GNLSE) that describes the propagation of intense femtosecond pulses through a fiber. The general form of the GNLSE for the slowly varying complex envelope $A(z,\tau)$ of a pulse centered at frequency ω_0 is given by

$$\begin{aligned}\frac{\partial A}{\partial z} &= -\frac{i}{2}\beta_2\frac{\partial^2 A}{\partial \tau^2} + \frac{1}{6}\beta_3\frac{\partial^3 A}{\partial \tau^3} + \frac{i}{24}\beta_4\frac{\partial^4 A}{\partial \tau^4} - \frac{\alpha}{2}A \\ &+ i\gamma|A|^2A - \frac{\gamma}{\omega_0}\frac{\partial\left(|A|^2A\right)}{\partial\tau} - i\gamma T_R A\frac{\partial|A|^2}{\partial\tau} \qquad (1)\end{aligned}$$

a pulse propagating along the z-axis within a retarded time frame $\tau = t - z/v_g$ with the group velocity v_g. The linear terms on the right-hand side of Eq. (1) represent the group velocity dispersion (GVD), namely second-order (SOD), third-order (TOD) and fourth-order (FOD) dispersion and the attenuation term corresponding to the

fiber loss α. The first nonlinear term represents self-phase modulation (SPM) with the nonlinear coefficient γ, which results from the intensity-dependent refractive index. The term proportional to γ/ω_0 results from the intensity dependence of the group velocity and causes self-steepening and shock formation at the pulse edge. The last term regards the intrapulse Raman scattering and originates from the delayed response, which causes a self-frequency shift, where T_R is related to the slope of the Raman gain. For the numerical solution of Eq. (1) we use a standard de-aliased pseudospectral method. The integration is performed by an eighth-order Runge-Kutta integration scheme using adaptive stepsize control [8].

4 Pulse Splitting

Fig. (2) shows an example for the pulse compression scheme with increasing power. A pulse with a width of $T_0 = 2.1$ ps is launched into the HNLF at a laser wavelength of 1550 nm. Fig. (2a,b,c) show the measured and calculated spectra. To have a good agreement with the experiment all terms of Eq. 1 have to be regarded. Especially the fourth-order dispersion coefficient $\beta_4 = 1.5 \times 10^{-4} ps^2/km$ has to be taken into account. Fig. (2d,e,f) represent the calculated pulse shapes after the spectral broadening in the HNLF and the subsequent pulse compression in the SMF. The length of the compensation SMF has to be decreased with increasing peak power. The optimal length, where the pulse width is in a minimum, is found numerically. The pulses are compared with the ideal case, where all higher-order terms are neglected.

Fig. (2a,b) shows the spectral broadening process by SPM in the HNLF for $P_{IN} = 20$ dBm and $P_{IN} = 22.5$ dBm. The structure of the resultant spectra are mainly determined by SPM and show the typical multi-peak structure characteristics. The impact of the small group velocity dispersion is a slight reduction in the bandwidth of the broadened pulse. A small asymmetry induced by TOD can be observed. In the optimal compression scheme the combined action of normal dispersion and SPM results in a broadened parabolic pulse shape with an almost linear frequency chirp across it, which is ideal for a subsequent pulse compression (Fig. (2d,e,f) dashed line). For low input powers (below $P_{IN} = 20$ dBm) the higher-order terms are unimportant and the compression is close to optimum (Fig. (2d)). The contribution of TOD appears with increasing bandwidth. The spectral asymmetry is more pronounced for $P_{IN} = 22.5$ dBm, but SPM is still dominant. The pulse shape (Fig. (2e)) experiences an asymmetric temporal development with an enhanced transfer of power from the trailing portion of the pulse to the leading one. Even though the pulse is distorted by TOD and there is a strong deviation from the ideal parabolic pulse shape, the pulse is efficiently compressed in the SMF, which reflects still the linearity of the chirp. The strong pedestal of the compressed pulse results here from the FOD in the HNLF. The behavior changes with a further increase of the average power until a certain treshold is reached, where the evolution of the pulse changes dramatically. At $P_{IN} =$ 23.75 dBm the effect of SPM is no longer dominant for the characteristics of the

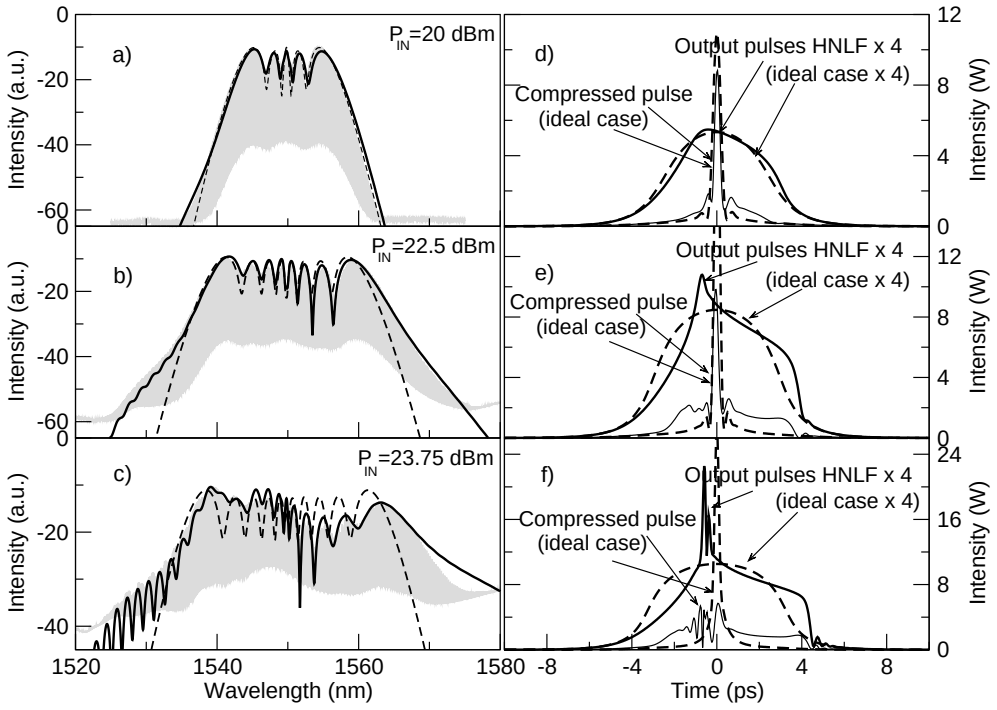

Figure 2: Measured (shaded) and calculated (lines) spectra after the HNLF for an average power P_{IN} of a) 20 dBm , b) 22.5 dBm c) 23.75 dBm. The solid curves show the calculated spectra, where all terms in Eq. (1) are taken into account. Calculated pulses after the HNLF and the subsequent pulse compression in the SMF with increasing average power P_{IN} of d) 20 dBm e) 22.5 dBm and f) 23.5 dBm. The dashed lines represent the numerical simulations for the ideal spectra and pulse shapes, where all higher-order effects are switched off.

spectrum; see Fig. (2c). The spectral wings are more pronounced than for the ideal propagation and a strong asymmetry can be observed with the blue side having more energy. The transmitted pulse in the HNLF exhibits an asymmetric splitting and the injection into the SMF leads not to the desired compression behavior anymore. From here the compression scheme fails completely, but turned into a considerably complicated situation. Further increase of power causes pulse shapes with multiple sub-pulse signature. Thus, this splitting represents a fundamental limit for pulse compression and suggests that operation below a critical power is necessary for optimal compression. The critical peak power for pulse splitting decreases with a decrease of the temporal width of the injected pulse.

The FROG measurements in Fig. (3) characterize the temporal profile and the frequency chirp near and above the point at which the pulse splits up and support qualitatively the pulse splitting scenario described above. At an average power of $P_{IN} = 22.0$ dBm the pulse exhibits a steep edge (i.e., an optical shock wave) at the leading portion (Fig. (3a)). A narrow peak is formed and an increase of the peak

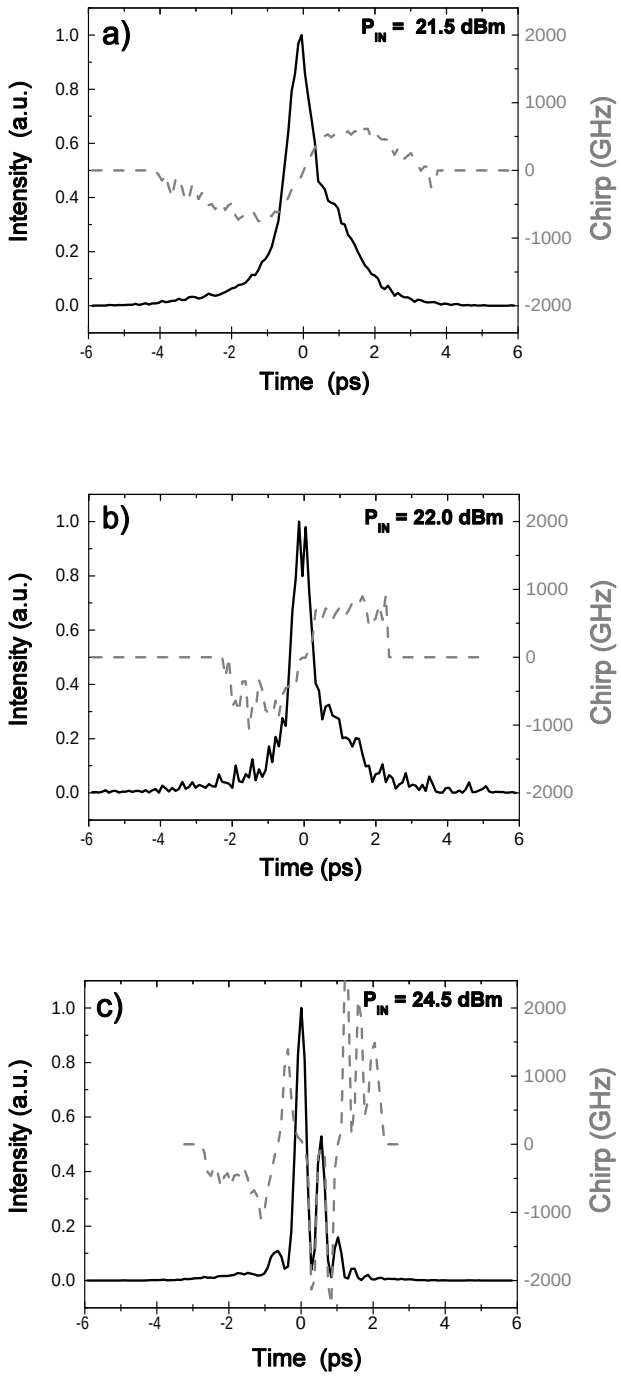

Figure 3: Pulse intensity (solid black line) and pulse chirp (dashed gray line) retrieved from FROG spectrograms for average powers P_{IN} of a) 21.5 dBm, b) 22.0 dBm and c) 24.5 dBm.

intensity at the front of the pulse can be observed. Numerical calculations, where we investigate successively each higher-order term (dispersion and nonlinearity) of the GNLSE separately, show, that this behavior has to be ascribed alone to the action of β_3. Below the point of pulse splitting there is no strong detrimental effect on the chirp's linear behavior (dashed gray line) by TOD. The frequency chirp within the pulse is still linear and the pulse can be used for a subsequent pulse compression. Also the distortion of the pulse can be compensated by an appropriate amount of negative TOD. Further propagation or a higher peak power is leading to a sharp increase of the peak intensity at the front of the pulse, which is halted by temporal pulse splitting (Fig. (3b)). The chirp is no longer linear within the pulse and shows a discontinuity. As the power is increased, the splitting occurs at decreasing values of z and after the initial splitting the pulse undergoes multiple splitting (Fig. (3c)). The observed phenomenon is similar to the behavior induced by self-focusing in nonlinear dispersive media for ultrashort pulses, where the effect of self-steepening is important [9, 10]. During the spatial collapse, both pulse steepening and asymmetric temporal pulse splitting of the pulse envelope are observed.

5 Conclusion

We have detected a fundamental compression limit for high-nonlinear dispersion-flattened fibers in the normal dispersion regime near the zero-dispersion regime. The desired generation of a broadband continuum by SPM is perturbated by already small TOD, which results in pulse splitting above a critical pulse power. This suggests that operation below that critical power is necessary for optimal pulse compression. The latter holds not only for the special fibers used here, but in general, wherever TOD interferes with SPM in the normal dispersion regime.

References

[1] K. R. Tamura and M. Nakazawa, "54-fs, 10-GHz soliton generation from a polarization-maintaining dispersion-flattened dispersion-decreasing fiber pulse compressor," *Opt. Lett.*, vol. 26, no. 11, pp. 762–754, 2001.

[2] K. R. Tamura and K. Sato, "50-GHz repetition-rate, 280-fs pulse generation at 100-mw average power from a mode-locked laser diode externally compressed in a pedestal-free," *Opt. Lett.*, vol. 27, no. 14, pp. 1268–1270, 2002.

[3] L. F. Mollenauer, R. H. Stolen, J. P. Gordon, and W. J. Tomlinson, "Extreme picosecond pulse-narrowing by means of soliton effect in single-mode optical fibers," *Opt. Lett.*, vol. 26, no. 11, pp. 289–291, 1983.

[4] K. C. Chan and H. F. Liu, "Effect of third-order dispersion on soliton-effect pulse compression," *Opt. Lett.*, vol. 19, no. 11, pp. 49–51, 1994.

[5] D. G. Ouzounov, C. H. Hensely, A. L. Gaeta, N. Venkateraman, M. T. Gallagher, and K. W. Koch, "Soliton pulse compression in photonic band-gap fibers," *Opt. Express*, vol. 12, no. 16, pp. 6153–6159, 2005.

[6] W. J. Tomlinson, R. H. Stolen, and C. V. Shank, "Compression of optical pulses chirped by self-phase modulation in fibers," *J. Opt. Soc. Am. B*, vol. 1, no. 2, pp. 139–149, 1984.

[7] J. M. Dudley, L. P. Barry, P. G. Bollond, J. D. Harvey, R. Leonhardt, and P. D. Drummond, "Direct measurement of pulse distortion near the zero–dispersion wavelength in an optical fiber by frequency–resolved optical gating," *Opt. Lett.*, vol. 22, no. 7, pp. 457–459, 1997.

[8] A. Demircan and U. Bandelow, "Supercontinuum generation by the modulation instability," *Opt. Comm.*, vol. 244, no. 1-6, pp. 181–185, 2005.

[9] J. K. Ranka and A. L. Gaeta, "Breakdown of the slowly varying envelope approximation in the self-focusing of ultrashort pulses," *Opt. Lett.*, vol. 23, no. 7, pp. 534–536, 1998.

[10] A. L. Gaeta, "Catastrophic collapse of ultrashort pulses," *Phys. Rev. Lett.*, vol. 85, no. 16, pp. 3582–3585, 2000.